In Situ Observation of NaCl Crystal Growth by the Vapor Diffusion Method with a Mach—Zehnder Interferometer

2011 Chinese Phys. Lett. 28 108102

(http://iopscience.iop.org/0256-307X/28/10/108102)

In Situ Observation of NaCl Crystal Growth by the Vapor Diffusion Method with a Mach–Zehnder Interferometer *

ZHAO Jing(赵静)[1], MIAO Hong(缪泓)[1**], DUAN Li(段俐)[2], KANG Qi(康琦)[2], HE Ling-Hui(何陵辉)[1]

[1]*Key Laboratory of Mechanical Behavior and Design of Materials, Department of Modern Mechanics, University of Science and Technology of China, Hefei 230027*

[2]*National Microgravity Laboratory, Institute of Mechanics, Chinese Academy of Sciences, Beijing 100190*

(Received 24 January 2011)

Vapor diffusion experiments with different thicknesses of oil barriers are observed by a real-time optical diagnostic system consisting of a Mach–Zehnder interferometer, a microscope and an image processor. Spatiotemporal analysis is first employed to extract the absolute concentration evolution and supersaturation during the entire crystallization process. The nucleation and crystal growth processes are then analyzed. It is found that the crystallization process can be easily classified into four stages in our experiments, according to the analysis of interferograms and the absolute concentration curve. This can help us understand the details of crystal growth. The rule of quality change of crystals with increasing thickness of oil barriers is also analyzed, and could be interpreted by the absolute concentration variation and crystallization phase diagram.

PACS: 81.10.Dn, 42.30.Rx DOI:10.1088/0256-307X/28/10/108102

The growth of large crystals with a high degree of perfection is essential in the chemical industry and the protein field. Vapor diffusion[1] is the most widely used technique in protein crystallization, the principle of which is that the solution gradually reaches saturation and then starts to crystallize through diffusion or evaporation. It is a challenge to know the precise status of nucleation and supersaturation evolution in vapor diffusion experiments[2] because they are affected by both water vaporization and crystal growth. Vapor diffusion also suffers from a common problem, i.e. the production of showers of small crystals instead of single, large ones. This is probably because the process of crystallization takes place too rapidly. To slow down the crystallization process and control evaporation rates, Chayen[3] presented an approach that employs an oil barrier over the reservoir of conventional vapor diffusion trials. The effect of different evaporation rates on crystal quality has been qualitatively discussed before,[3,4] but quantitative analysis was rarely carried out. Therefore, it is necessary to develop diagnostic and monitoring experiments to investigate the crystal growth kinetics of vapor diffusion and the influence of different evaporation rates on the crystallization process.

Over the past few decades, many studies have been carried out on crystal growth kinetics,[5] mass transfer[6] and the crystallization phase diagram.[2] However, current non-invasion techniques applied in the research of crystal growth, such as Raman spectroscopy,[7] near-infrared spectroscopy[8] and holographic interferometer,[9] including real-time phase-shift interferometry,[6,10] cannot accurately obtain the absolute concentration, but only the relative spatial concentration at a certain instant. Recently, spatiotemporal analysis,[11] a novel technique that can extract phase variation along the time axis, was proposed and successfully applied to investigate dynamic processes from a sequence of digital holograms,[12,13] speckle patterns[14] and non-interferometric fringe patterns.[15] In this Letter, to investigate the crystal growth kinetics of vapor diffusion, the method is first employed to extract the spatial and temporal phase, which can be transformed to absolute concentration and supersaturation directly. Furthermore, the influence of different evaporation rates on crystal quality is also studied.

Crystallization experiments with different thicknesses of oil barriers (0, 0.06, 0.095, 0.12, 0.14 and 0.175 mm) were conducted by evaporation that was similar in principle to vapor diffusion. The unsaturated solution gradually reaches supersaturation, and spontaneous nucleation will happen when the supersaturation reaches a certain value. Then these nuclei can grow into crystals of visible sizes in this supersaturated system.

The crystallization process was real-time monitored with a modified Mach–Zehnder interferometer, as shown in Fig. 1. The light source is a He-Ne laser of wavelength 632.8 nm. The interferograms are magnified by a microscope objective and recorded by a CCD camera with a pixel size of $9.9 \times 9.9\,\mu m^2$. The initial concentration of NaCl solution was 24.24%, which was prepared at 20℃. The dimensions of the sample cell

*Supported by the National Natural Science Foundation of China under Grant Nos. 11072235 and 10732080, and the National Basic Research Program of China under Grant No. 2007CB936803.

**Correspondence author. Email: miaohong@ustc.edu.cn

are $14 \times 6 \times 12\,\text{mm}^3$. The interferograms can be automatically and continuously grabbed by setting the image grab interval to one frame per minute. The total experimental times ranged from 7 to 14 h, corresponding to different oil barrier thicknesses.

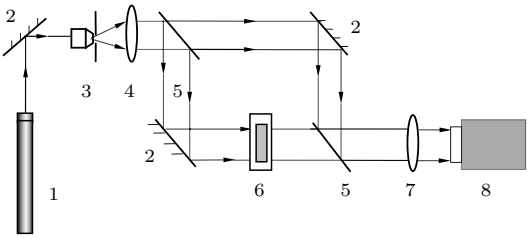

Fig. 1. The experimental setup of the interferometry. 1: He-Ne Laser; 2: mirror; 3: spatial filter; 4: collimation lens; 5: beam splitter; 6: growth cell; 7: imaging lens; 8: CCD.

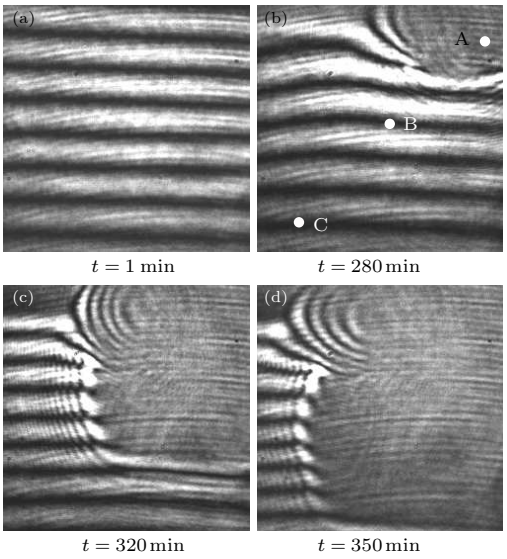

Fig. 2. The sequence of interferograms during the crystallization process captured by CCD. The three points, A, B and C, marked in (b) represent nucleation, crystal growth and solution, respectively.

The absolute concentration evolution is measured by spatiotemporal analysis,[11] which determines the instantaneous refractive index of solution by analyzing the intensity variation of interference speckle along the time axis, pixel by pixel. The Fourier transfer method with a band-pass filter is usually applied to extract the refractive index evolution from the temporal signal of each pixel. The relationship between the refractive index and the concentration of NaCl solution measured by the WAY-15 ABBE refractometer can be written as $c = 5.3899n - 7.1852$, where c and n represent the concentration and refractive index of the solution, respectively.

The interferograms of the crystallization process were recorded by a CCD camera in temporal sequence, as shown in Fig. 2. Changes in fringe spacing denoted the variations of the concentration gradient, and the direction the fringes moved depended on an increase or decrease in the absolute concentration of the solution. As soon as the experiment began, interference fringes moved up uniformly until crystal nucleation, then crystal appeared at the upper section of the solution at about 278 min. Subsequently, the fringes thickened and moved in the opposite direction with the growth of the crystal. Finally, the fringes became thinner and gradually became more static.

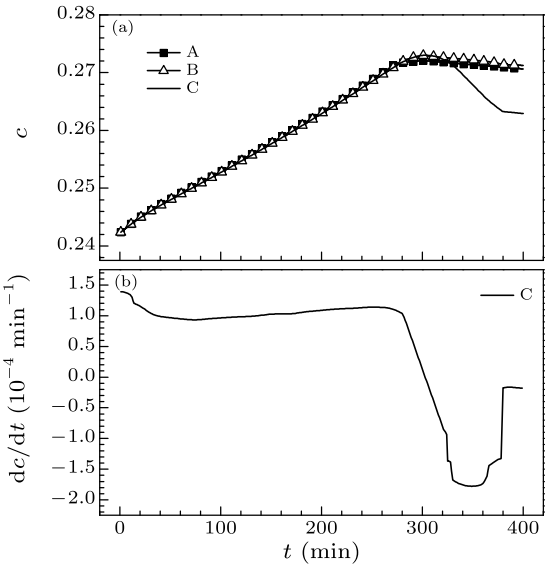

Fig. 3. (a) The evolution of the absolute concentration of the three points A, B and C marked in Fig. 2(b). (b) The concentration variance velocity of point C.

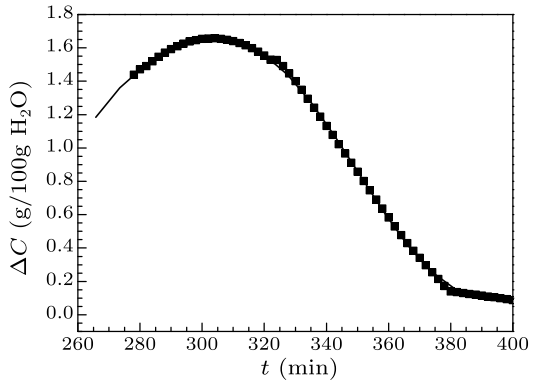

Fig. 4. The supersaturation curve during the nucleation and growth stages.

Since the refractive indices of the crystal and solution are different, the laser beam passing through the crystal-liquid interface will be scattered. Corresponding to the interferogram, the interference fringes where the crystal appears will be distorted. On the contrary, the area in which no crystal exists is always covered by straight interference fringes. In Fig. 2(b), points A, B and C were selected to represent the nucleation, growth and solution, respectively. Figure 3(a) shows the absolute concentration curve of these three points, which were extracted by spatiotemporal anal-

ysis. The concentration curves of points A and B are constant after being covered by crystal. Curve C denoted the concentration evolution of the solution, because point C was full of solution through the crystallization process. The concentration change rate (which indirectly denotes the evaporation rate) could be obtained from the concentration curve of point C, as shown in Fig. 3(b).

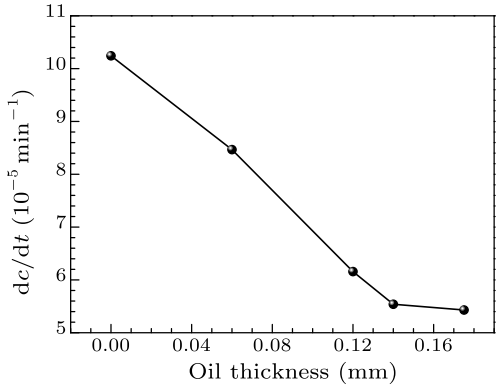

Fig. 5. The evaporation rates versus the thickness of oil barriers (0, 0.06, 0.12, 0.14 and 0.175mm).

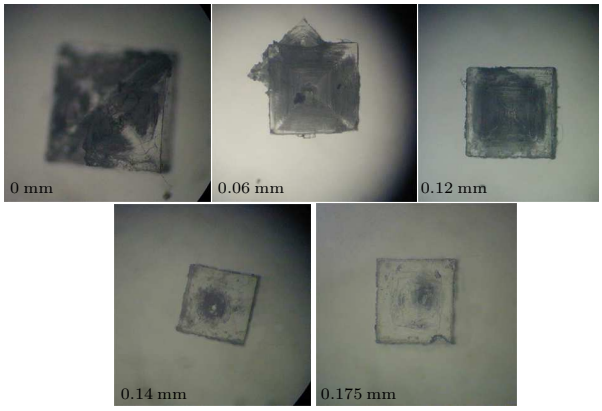

Fig. 6. Optical micrographs of crystals growing under different thicknesses of oil barrier (0, 0.06, 0.12, 0.14 and 0.175mm).

From the absolute concentration curve C, supersaturation after nucleation ($\Delta c = c - c^*$, where c^* is the solubility), which is the driving force of crystal growth, could be calculated easily as shown in Fig. 4. It is shown that the stable crystal nucleus was formed when absolute supersaturation reached 1.43945 (g/100gH_2O) in this experiment. Afterwards, supersaturation increases to the maximum when $t =$ 304 min and then decreases to the equilibrium.

Figure 5 shows the rates of concentration variance before nucleation with different thicknesses of oil barriers, which can be obtained from the velocity curve of concentration variance as shown in Fig. 3(b). The results indicate that the rates of concentration variance (namely the evaporation rates) decrease quickly with the increase in oil thickness, and then the decrease rates become slower. The micrographs of crystals grown under different oil thicknesses are shown in Fig. 6. This demonstrates that crystal quality has been improved with the increase in oil thickness.

In general, according to the changes in the fringes after analysis of the sequence of interferograms (Fig. 2) and concentration curves (Fig. 3(a)), the crystallization process of vapor diffusion can be classified easily into four stages: (1) the solution evaporation stage, in which the unsaturated solution gradually reaches supersaturation; (2) the crystal nucleation stage, in which crystals appear in the upper section of the solution and the concentration gradient begins to alter, (3) the crystal growth stage, in which the boundary layer,[6] convection[16] and other phenomena could usually be observed due to mass exchange (most research was focused on this stage in the past few years); and (4) the completion stage, in which the concentration gradient becomes smaller and gradually tends to be static.

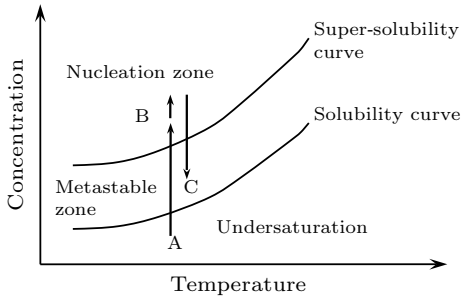

Fig. 7. Crystallization phase diagram of vapor diffusion.

From the supersaturation curve during the nucleation and growth stages, as shown in Fig. 4, it is found that only NaCl crystals can nucleate spontaneously when the solution is supersaturated. In this experiment, when the absolute supersaturation reached 1.43945 (g/100gH_2O), a stable nucleus can be found near the evaporating surface. This is because the crystallization process is an orderly process, which means that molecules in a random state in the solution were embedded into an ordered solid phase. The formation of a new phase (crystal) requires a certain degree of supersaturation to overcome surface free energy in order to generate a solid-liquid interface. Since the supersaturation when nucleation can be obtained, the nucleation kinetics parameters,[17] such as the critical radius ($r_c = \frac{2\sigma\nu}{RT\ln s} = 30\,\text{nm}$), and the maximum Gibbs free energy ($\Delta G_{\max} = \frac{16\pi\sigma^3\nu^2}{3R^2T^2\ln^2 s} = 7.9\times10^{-16}\,\text{J}$), can be calculated, where σ, ν, R, and T are the interfacial tension, molar volume of the crystals, gas constant and temperature, respectively, and $s = c/c^*$. It is also worth noting that supersaturation still increases after the crystal nucleus appears because water evaporation is faster than crystal growth. In contrast, when the crystal growth rate is larger than the water evapora-

tion rate, supersaturation decreases after $t = 304$ min.

Figure 7 shows the crystallization phase diagram,[18] which provides a method for quantifying the influence of concentration, temperature, etc, on the production of crystals. Areas A and B denote the unsaturated area and spontaneous nucleation area, respectively. The metastable zone is the area where good-quality crystals can grow. In this area, spontaneous nucleation cannot happen without seed crystals, unless concentration reaches the nucleation zone. Since the experiments are conducted by evaporation at a constant temperature, the line from A to B, which represents the concentration increase with the evaporation of solvent, is perpendicular to the temperature axis. After nucleation, the concentration curve still rises for some time to reach maximum supersaturation. The dotted line denotes the decrease in concentration at the same temperature as the crystal growth rate exceeds the evaporation rate, which corresponds to the decrease part of the absolute concentration, as shown in Fig. 3(a). Based on the concentration evolution and the crystallization phase diagram, it is better for the concentration to return to the metastable zone once stable nuclei have been formed in the nucleation zone. When the oil barrier is covered on the solution, the evaporation rate becomes slow, as shown in Fig. 5. The maximum supersaturation will be smaller when the corresponding oil barrier is thicker. The concentration is easier to decline to the metastable zone. Consequently, slowing down the water vaporization rate can be a means to control crystal quality. The results of experiments with different oil barriers also confirm that crystal quality is improved with a decrease in water vaporization rates induced by the increasing oil thickness, as shown in Figs. 5 and 6.

In summary, vapor diffusion experiments with different thicknesses of oil barriers have been carried out with a real-time optical diagnostic system. The kinetic parameters of vapor diffusion, such as absolute concentration, supersaturation and evaporation rate, through the entire crystallization process are obtained by a spatiotemporal analysis of interferograms. The quantitative analysis of the relationship between crystal quality and evaporation rate is discussed. The results show that the crystallization process can be classified into four stages. The evaporation rate decreases and crystal quality is improved with increasing oil barrier thickness. This can be interpreted by analysis of the absolute supersaturation and crystallization phase diagram.

References

[1] McPherson A 2004 *Methods* **34** 254
[2] Saridakis E E G, Shaw Stewart P D, Lloyd L F and Blow D M 1994 *Acta Cryst.* D **50** 293
[3] Chayen N E 1998 *Acta Cryst.* D **54** 8
[4] Li G, Xiang Y, Zhang Y and Wang D C 2001 *J. Appl. Cryst.* **34** 388
[5] Snell E H, Helliwell J R, Boggon T J, Lautenschlager P and Potthast L 1996 *Acta Cryst.* D **52** 529
[6] Duan L, Kang Q, Hu W R, Li G P and Wang D C 2002 *Biophys. Chem.* **97** 189
[7] Zhang X, Yin S T, Wan S M, You J L, Chen H, Zhao S J and Zhang Q L 2007 *Chin. Phys. Lett.* **24** 1898
[8] Olesberg J T, Arnold M A, Hu S Y and Wiencek J M 2000 *Anal. Chem.* **72** 4985
[9] Chen W C, Shen Y X, Ma W Y, Li M and Chen Y S 1991 *Chin. Phys. Lett.* **8** 469
[10] Onuma K, Nakamura T and Kuwashima S 1996 *J. Cryst. Growth* **167** 387
[11] Qian K, Fu Y, Liu Q, Seah H S and Asundi A 2006 *Opt. Lett.* **31** 2121
[12] Fu Y, Pedrini G and Osten W 2007 *Appl. Opt.* **46** 5719
[13] Fu Y, Shi H and Miao H 2009 *Appl. Opt.* **48** 1990
[14] Miao H, Gu P, Liu Z T, Liu G, Wu X P and Zhao J H 2005 *Opt. Lasers Eng.* **43** 885
[15] Tay C J, Quan C, Fu Y, Chen L J and Shang H M 2004 *Opt. Laser Technol.* **36** 471
[16] Duan L and Shu J Z 2001 *J. Cryst. Growth* **223** 181
[17] Sankar R, Raghavan C M and Jayavel R 2006 *Cryst. Res. Technol.* **41** 919
[18] Mitchell N A and Frawley P J 2010 *J. Cryst. Growth* **312** 2740